

## Optical studies of the charge transfer complex in polythiophene/fullerene blends for organic photovoltaic applications

T. Drori,<sup>\*</sup> J. Holt,<sup>†</sup> and Z. V. Vardeny<sup>‡</sup>*Department of Physics and Astronomy, University of Utah, Salt Lake City, Utah 84112, USA*

(Received 3 April 2010; revised manuscript received 26 June 2010; published 12 August 2010)

We studied the photophysics of regioregular polythiophene/C<sub>61</sub> (RR-P3HT/PCBM) blend films utilized for organic photovoltaic applications using the femtosecond transient and steady-state photomodulation techniques with above-gap and below-gap pump excitations and electroabsorption spectroscopy. We provide strong evidence for the existence of charge transfer complex (CTC) state in the blend that is formed deep inside the optical gap of the polymer and fullerene constituents, which is clearly revealed in the electroabsorption spectrum with an onset at 1.2 eV. We identify this “midgap” band as the lowest lying CTC state formed at the interfaces separating the polymer and fullerene phases. With above-gap pump excitation the primary photoexcitations in the blend are excitons and polarons in the polymer domains that are generated within the experimental time resolution (150 fs), having distinguishable photoinduced absorption (PA) bands in the mid-IR. The photogenerated excitons subsequently decay within  $\sim 10$  ps, consistent with the polymer weak photoluminescence in the blend. In contrast, with below-gap pump excitation, a new PA band in the mid-IR is generated within our time resolution, which is associated with photogenerated species that decay into polarons at much later times; also no PA of excitons is observed. We interpret the photoexcitations as CT excitons, which with below-gap pump excitation are resonantly generated on the CTC states at the interfaces, as the first step for polaron generation, without involving intrachain excitons in the polymer phase. We found that the polarons generated with below-gap pump excitation are trapped at the interfaces with relatively long lifetime, and thus may generate polarons on the polymer chains and fullerene molecules with a different mechanism than with above-gap excitation. In any case the interfacial polarons generated with below-gap excitation do not substantially contribute to the photocurrent density in photovoltaic applications because of the relatively thin active layer using the traditional bulk heterojunctions design. This is shown by comparing the charge photogeneration efficiency spectrum measured on a fabricated photovoltaic solar cell with the polaron photogeneration action spectrum measured on a thick blend film.

DOI: [10.1103/PhysRevB.82.075207](https://doi.org/10.1103/PhysRevB.82.075207)

PACS number(s): 78.40.Me, 78.40.Pg, 78.47.J-, 78.40.Fy

### I. INTRODUCTION

The most efficient organic photovoltaic (OPV) cells to date are based on bulk heterojunctions (BHJ) of  $\pi$ -conjugated polymer/fullerene composite blends<sup>1–7</sup> that show phase separation of the polymer and fullerene constituents,<sup>3</sup> having power-conversion efficiency (PCE) up to 7.4%.<sup>8</sup> The mechanism of charge separation in polymers that are lightly doped with fullerene has been traditionally considered to be a single-step electron transfer from the photoexcited polymer chain onto the fullerene acceptor molecule.<sup>9,10</sup> In more heavily doped polymer (namely, blend) films it has been proposed that an interfacial dipole formation at the donor-acceptor interface assists charge separation.<sup>11</sup> However a series of recent reports have indicated that the photoinduced charge-separation process in the blend involves one or more intermediate steps.<sup>12–17</sup> One such step may involve a charge transfer complex (CTC) state that is formed at the interface between the polymer and fullerene phases in the blend.<sup>14,17</sup> Evidence for a CTC intermediate state has been reported in various donor/acceptor blends.<sup>18–24</sup> Such a CTC state has been supported theoretically;<sup>25–28</sup> and its important role in the charge-generation process in the blend,<sup>19,24</sup> and open circuit voltage in OPV cells based on BHJ configuration has been recognized.<sup>29</sup>

In our previous work we investigated the CTC state in poly(phenylene vinylene)/C<sub>60</sub> blend,<sup>19</sup> as well as poly(phenylene vinylene)/2,4,7-trinitro-9-fluorenone (TNF) blend;<sup>23</sup>

but OPV cells based on these blends do not show high PCE.<sup>30</sup> In the present work we study the CTC state in the important blend of regioregular (3-hexylthiophene-2,5-diyl) (RR-P3HT, Fig. 1 inset) and<sup>6</sup> poly-phenyl-C<sub>61</sub> butyric acid methyl ester (PCBM-C<sub>61</sub>, Fig. 1 inset); this blend is the active layer of one of the most efficient OPV cells to date.<sup>2,31</sup> In this blend we show the existence of a CTC state with onset at  $\hbar\omega \sim 1.2$  eV, which is deep inside the optical gap of the material constituents, by employing transient and steady-state photomodulation (PM) spectra excited with both below-gap and above-gap photon energies and electroabsorption (EA) spectroscopy. The most direct evidence for the CTC state is provided here by the EA spectroscopy that reveals a midgap optical feature with an onset at  $\hbar\omega \sim 1.2$  eV. From the transient PM spectra of the blend we conclude that above-gap pump excitation creates excitons and polarons in the polymer phase within the experimental time resolution (150 fs). But below-gap pump excitation gives rise to a photoinduced absorption (PA) band in the mid-IR, which we interpret as due to photogenerated CT excitons on the CTC states that are resonantly generated.<sup>28</sup> The resonant CT excitons are instantaneously generated and subsequently decay into polarons on the polymer chains and fullerene molecules at much later time. The steady-state PM spectra show that it is indeed possible to generate polarons on the polymer chains and fullerene molecules with below-gap excitation without

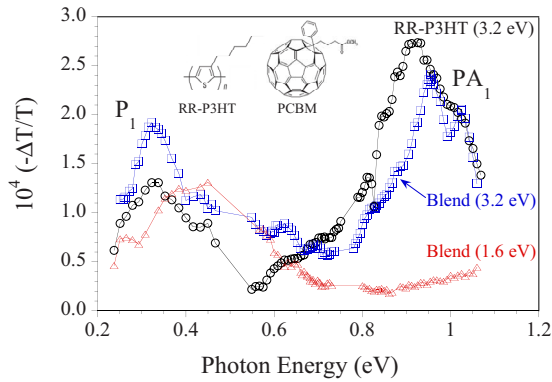


FIG. 1. (Color online) Transient PM spectra at  $t=0$  in pristine RR-P3HT film pumped at 3.2 eV (black circles), and blend film pumped at 3.2 eV (blue squares) and 1.6 eV (red triangles); for better comparison, the below-gap curve has been scaled by 0.7.

the need of photogenerated intrachain excitons as the first state preceding charge separation. The below-gap-generated polarons are trapped close to the polymer/fullerene interfaces and hardly contribute to the photocurrent density in solar-cell devices because of the device's relatively thin active layer.<sup>19</sup> This was verified by measuring the internal PCE (IPCE) spectrum in a neat OPV cell based on BHJ of this blend in comparison with the polaron action spectrum of a blend thick film.

## II. EXPERIMENTAL

The mixing ratio of the RR-P3HT/PCBM blend that we used in our investigations was 1.2:1 by weight, which gives the optimal power-conversion efficiency in OPV cells application<sup>2</sup> when the regioregularity of the RR-P3HT polymer constituent is high.<sup>3</sup> The PCBM and RR-P3HT powders were supplied by Plextronics, Inc. The films used for the optical measurements were prepared either by spin casting or drop casting onto an optical transparent substrate such as sapphire or CsI, depending on the spectral range of interest. For the polaron action spectrum we used a drop cast film  $\sim 20 \mu\text{m}$  thick. Subsequently the films were thermally annealed at  $150^\circ\text{C}$  for 3 min. The films were then put into a variable temperature cryostat under dynamic vacuum of  $\sim 10^{-4}$  torr, which was also used to prevent photooxidation that is enhanced by the applied laser illumination. Atomic force microscopy<sup>32</sup> and resonance Raman spectroscopy studies<sup>33</sup> have shown that phase-separated domains of aggregated polymer chains and fullerene molecules are formed in this blend, especially after the film undergoes an annealing process at elevated temperature.<sup>24</sup> The domain size of these aggregates is ideally on the scale of the exciton diffusion length ( $\sim 10 \text{ nm}$ ), which enables excitons to reach the donor/acceptor interface before recombination occurs.<sup>34–36</sup>

For the OPV cells we used high-quality RR-P3HT polymer with regioregularity higher than 99%, molecular weight  $M_n=58 \text{ kDa}$ , and polydispersivity of  $\sim 1.76$ . The blend in solution was spin cast on a hole transport layer that was predeposited onto a low-resistance indium tin oxide (ITO) substrate. The film thickness was about 200 nm and was

capped by a 10 nm Ca/100 nm Al cathode. The  $I$ - $V$  characteristics of the encapsulated devices were measured in air using a Keithley 2000 multimeter under simulated  $100 \text{ mW/cm}^2$  AM1.5 illumination that was provided by a 300 Watt Oriol solar illuminator. Light intensity was tuned using KG-5 filtered Si reference cell calibrated at NREL. Efficiency values were corrected by a spectral mismatch factor that was measured using a KG-5 color-filtered reference cell. The IPCE spectrum was measured using an automated electric quantum efficiency system from Custom Systems Integration, Inc. Special care was taken to calibrate the IPCE spectrum against a precalibrated Hamamatsu Si photodetector using a set of order-sorting filters. We also verified that the IPCE spectrum convoluted with the solar illumination power indeed gives the same PCE as that calculated from the  $I$ - $V$  characteristics. All the OPV cell fabrication was done in a nitrogen-filled glove box, where the oxygen and moisture level was kept below 0.1 ppm.

The transient PM spectroscopy was utilized to resolve the primordial charge generation steps in the blend film. Specifically, we used the femtoseconds (fs) two-color pump-probe correlation technique with a low-power (energy/pulse  $\sim 0.1 \text{ nJ}$ ), high repetition rate ( $\sim 80 \text{ MHz}$ ) laser system based on Ti:sapphire (Tsunami, Spectra-Physics) having a temporal pulse resolution of 150 fs. In this technique the time evolution of the photoexcitations is monitored by the excited-state absorption of the photogenerated species, where the time,  $t$ , is set by a computerized delay line (or translation stage) between the pump and probe pulses with  $\sim 0.1 \text{ fs}$  time resolution. The pump photon energy,  $\hbar\omega$ , was set at 1.55 eV for below-gap excitation or frequency doubled to  $\hbar\omega = 3.1 \text{ eV}$  for above-gap excitation. We used the output beam of an optical parametric oscillator (OPO) (Opal, Spectra-Physics) as a probe with  $\hbar\omega$  ranging from 0.24 to 1.1 eV, which was generated by tuning the OPO beams of the “signal,” “idler,” and their difference frequency obtained in a nonlinear crystal.<sup>37</sup> The pump and probe beams were focused on the film surface inside the cryostat by means of a telescopic microscope to a spot  $\sim 50 \mu\text{m}$  in diameter; and the “beam-walk” known to exist in pump/probe correlation spectroscopy measurements was carefully minimized. The transient PM signal was measured using a phase sensitive lock-in technique at modulation frequency,  $f=30 \text{ kHz}$  provided by an acousto-optic modulator. In the mid-IR spectral range of interest that we focus on here we only obtained PA, which is given as the fractional change in transmission,  $T$ , namely,  $-\Delta T/T(t)$ . Both  $T$  and  $\Delta T$  were measured by solid-state photodetectors such as Ge, InSb, and MCT depending on the spectral range. No photoluminescence was observed in the mid-IR spectral range with the RR-P3HT/PCBM blend.<sup>24</sup>

We used the cw PM spectroscopy to study the long-lived photoexcitations in the blend, again with pump excitation,  $\hbar\omega$  above gap and below gap relative to the optical gap of the blend constituents. The steady-state PM spectrum was measured using a standard setup;<sup>37</sup> for above-gap excitation we used an  $\text{Ar}^+$  laser beam at  $\hbar\omega=2.5 \text{ eV}$  whereas for below-gap excitation we used a Ti-sapphire laser beam at  $\hbar\omega=1.55 \text{ eV}$  and a He-Ne laser at  $\hbar\omega=1.96 \text{ eV}$ . The pump beam was modulated at various frequencies,  $f$ , by a chopper. A beam from an incandescent tungsten/halogen lamp was

used as the probe. The PM signal was measured using a lock-in amplifier referenced at  $f$ , a monochromator, and various combinations of gratings, filters, and solid-state photodetectors (Si, Ge, and InSb) that span the spectral range  $0.3 < \hbar\omega(\text{probe}) < 2.7$  eV;<sup>38</sup> or, alternatively averaging 6000 scans of pump excitation turned “on” and “off” using a Fourier transform infrared spectrometer for  $0.05 < \hbar\omega(\text{probe}) < 0.4$  eV.<sup>39</sup> We note that because of the extended probe spectral range in the steady-state PM spectrum, the spectrum also contains a photobleaching band with positive  $\Delta T/T$  for  $\hbar\omega(\text{probe}) > E_g$  (the polymer optical gap).

For the pump excitation used to obtain the action spectrum of the lower energy polaron PA band we utilized a xenon incandescent lamp, of which beam was modulated and dispersed through a second monochromator that was normalized to obtain the photogeneration response of polarons/incident photon. The polaron action spectrum was measured at a fix probe  $\hbar\omega$  in the spectral range of  $0.25 < \hbar\omega < 0.5$  eV (obtained using a long-pass filter on the Tungsten lamp beam<sup>19</sup>). In order to retrieve the mean polaron lifetime,  $\tau$ , that is necessary for normalizing the polaron action spectrum (see below), the frequency response of both in-phase and quadrature PA components were measured, and fit to an equation of the form

$$\Delta T(f)/T = G\tau[1 + (i2\pi f\tau)^p], \quad (1)$$

where  $G$  is the generation rate (proportional to the laser intensity) and  $p$  ( $< 1$ ) is the dispersive parameter that describes the recombination dispersion of polarons due to disorder in the system.<sup>40</sup>

The EA spectrum was obtained by measuring the electric field-induced  $\Delta T/T$  using a lock-in amplifier set at  $2f$  due to the field modulation at  $f$ ; where the film was deposited on a specially designed substrate that contained interdigitated electrodes.<sup>41</sup> For comparison we measured the EA spectra of both pristine polymer and fullerene films first, before measuring the EA in the blend. Special attention was given to the EA signal at spectral range below the optical gap of the blend material constituents.

### III. RESULTS AND DISCUSSION

#### A. Transient photomodulation spectroscopy

Figure 1 compares the transient PM spectra at time “ $t=0$ ” of three cases: pristine RR-P3HT pumped above gap at 3.1 eV and the 1:1.2 blend of RR-P3HT/PCBM pumped at both above gap at 3.1 eV and below gap at 1.55 eV. The PM spectrum of the blend was normalized by a factor of 0.7 for ease of comparison. Two prominent PA bands are evident in the pristine polymer. These are:  $PA_1$  at 0.93 eV that was previously assigned to optical transitions related to the photogenerated singlet intrachain excitons,<sup>42</sup> and  $P_1$  at 0.34 eV that was ascribed before as due to the lower energy polaron optical transition.<sup>43</sup> There is some structure to  $PA_1$ ; namely, a shoulder at  $\sim 1.0$  eV. The cause of this splitting is currently unknown,<sup>44</sup> but we recognize that such  $PA_1$  split was already observed in pristine RR-P3HT film before.<sup>37</sup> The relative intensity ratio  $P_1/PA_1$ , which has been traditionally used<sup>37</sup> to

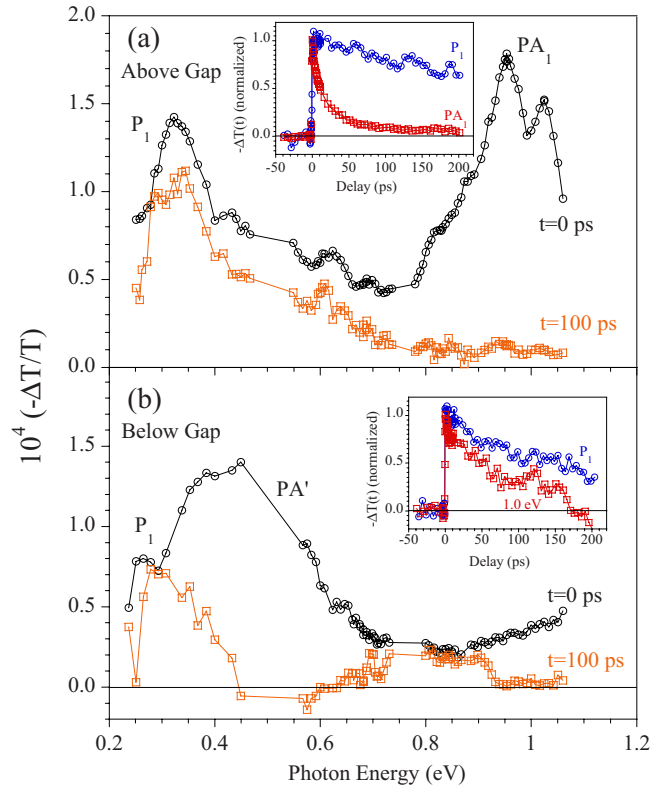


FIG. 2. (Color online) Comparison of PM transient spectra of RR-P3HT/PCBM blends at  $t=0$  (black circles) and 100 ps (orange squares) pumped at (a) 3.2 eV (above-gap) and (b) 1.6 eV (below-gap). The insets show transient  $PA_1$  (red squares) and  $P_1$  (blue circles) population decays.

estimate the branching ratio,  $\eta$ , of photogenerated polarons/excitons, can be calculated by integrating the area under each respective band. Using this method, and assuming that the majority of  $P_1$  is represented in Fig. 1, we obtain  $\eta=35\%$  in the pristine polymer, in good agreement with the literature value.<sup>37</sup> For the blend excited with above-gap pump we found that  $\eta$  is higher, since  $P_1/PA_1$  is larger (Fig. 1). This shows that the initial polaron photogeneration density is larger in the blend, probably because of larger disorder and impurity density in the polymer phase domains that interfere with the lamellae formation.<sup>45</sup> We note that  $PA_1$  for excitons is *absent* in the blend when exciting with below-gap pump; since the lowest exciton level in the polymer, namely, the  $1B_u$  at 1.95 eV is above the pump photon energy (see also Ref. 19).

The PM spectra of the blend when excited both above- and below-gap pump excitations at  $t=0$  ps and  $t=100$  ps, respectively, and the transient PA decays are presented in Fig. 2. When excited above the gap, the time traces of  $P_1$  [inset of Fig. 2(a)] reveal that it is created within 150 fs along with the primary singlet excitons, but its dynamics are much slower than those of the exciton  $PA_1$  band. Additionally, we emphasize that the populations of these two species appear to be *unrelated*; that is,  $P_1$  does not grow at the expense of  $PA_1$  decay. This is surprising, since the photogenerated exciton in the polymer phase should dissociate upon arriving by diffusion to the polymer/fullerene interfaces. Ap-



parently, even though the excitons arrive to the polymer/fullerene interface in about  $\tau=10$  ps, extra polaron generation in the polymer does not occur in the time domain of our experiment ( $\sim 500$  ps). We thus conclude that another mechanism needs to be found to explain the *delayed charge-dissociation* mechanism in P3HT/PCBM blend that we have revealed here.

We note that the 10 ps decay dynamics of the photogenerated excitons that we obtain in the blend is consistent with the delayed charge-generation inferred from picosecond spectroscopy in the visible/near-IR spectral range,<sup>36</sup> and also with the photoluminescence quantum efficiency,  $\mu$ , that we measured in the blend films using an integrated sphere.<sup>46</sup> We measured  $\mu < 1\%$  in the blend whereas  $\mu \sim 8\%$  for the pristine polymer. Since the radiative time,  $\tau_{\text{rad}}$ , of excitons in  $\pi$ -conjugated polymers was estimated to be  $\sim 1$  ns,<sup>47</sup> one can readily calculate  $\mu$  using the relation

$$\mu = \tau / \tau_{\text{rad}}. \quad (2)$$

Using Eq. (2) with  $\tau=10$  ps and  $\tau_{\text{rad}}=1$  ns we get  $\mu=1\%$  in excellent agreement with the actual cw obtained  $\mu$ .

As expected, no excitons are photogenerated on the polymer chains with below-gap excitation at  $\hbar\omega=1.55$  eV (Figs. 1 and 2). However, a band similar, but not exactly the same as  $P_1$ , which we call  $PA'$  is obtained with below-gap excitation. Its dissimilarity is marked by its peak at 0.45 eV, that is substantially blueshifted and broader than  $P_1$  formed with above-gap excitation. However, spectral decay indicates that until  $t=100$  ps  $PA'$  redshifts by  $\sim 150$  meV to a new band, that is very similar to that of  $P_1$  created with above-gap excitation (Fig. 1). This transient redshift may indicate that the band  $PA'$  precedes the creation of polarons on the polymer chains ( $P_1$ ).

The below-gap dynamics of  $PA'$  at 0.45 eV and at  $\hbar\omega(\text{probe})=1.0$  eV (where  $PA_1$  should have occurred with above-gap pump) are shown in Fig. 2(b) inset. The first 10 ps at  $\hbar\omega=1.0$  eV show a fast initial decay, after which the dynamics match those of  $PA'$ . The decay dynamics agree with the  $PA'$  redshift kinetics, and are thus related to the change in the photogenerated species character. We conclude that it is possible to generate localized polarons in the polymer chains using below-gap excitation of the blend. However this process proceeds in two steps. First there is an ultrafast formation of transient species that are different than the polaron excitations; these species subsequently dissociates into localized polarons in the polymer chains and fullerene molecules. This charge photogeneration process is viable in the blend and adds to the traditional dissociation process of photogenerated excitons at the polymer/fullerene interface.<sup>35</sup>

We speculate that the photogenerated transient species in the blend may be related to the CTC that is resonantly photogenerated with below-gap excitation. This type of excitation was recently identified to be a CT exciton at the polymer/fullerene interface.<sup>28</sup> We note that bound interfacial states, similar to the transient CT excitons obtained here have been previously identified in several polymer:polymer systems.<sup>48,49</sup> The CT exciton is composed of two components; namely, ionic and covalent. The ionic component is an electrostatic bound polaron pair with positive polaron on the

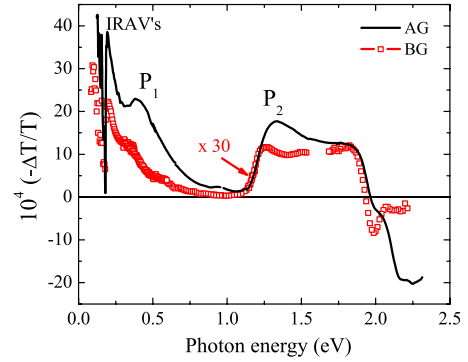


FIG. 3. (Color online) CW PA spectra of RR-P3HT/PCBM film using above gap (AG-black solid line) and below-gap (BG-red squares) pump excitation. The AG (BG) pump excitation  $\hbar\omega$  is 2.5 (1.55) eV. Both spectra show the known PA band signature of polarons; namely,  $P_1$ ,  $P_2$  bands and IRAV, as denoted.

polymer chain and negative polaron on the fullerene; whereas the covalent component involves hybridization via a transfer integral,  $t_{\perp}$ .<sup>24</sup> It has been predicted that the photogenerated CT exciton in polymer/fullerene blends has two prominent PA bands; one PA band in the mid-IR spectral range and the other PA band in the near-IR range.<sup>28</sup> We thus identify the transient  $PA'$  band obtained with below-gap excitation as due to the photogenerated CT excitons close to the polymer/fullerene interface, that further dissociate into charge polarons on the polymer chains and fullerene molecules within  $\sim 10$  ps. But these polarons are still electrostatically bound.

## B. Steady-state PM spectroscopy

A compelling signature of photogenerated charges in  $\pi$ -conjugated polymers is the appearance of in-gap polaron PA bands, as seen in the PM spectrum of the blend shown in Fig. 3. We clearly identify the well-known polaron PA bands  $P_1$  and  $P_2$ . In addition to the in-gap transitions, the polaron excitation also renormalizes the frequencies of the Raman-active amplitude modes in the polymer chain, where the small polaron mass causes the IR active vibrations (IRAV) to possess very large oscillator strengths.<sup>50</sup> Such IRAV indeed accompany the polaron PA bands in the blend as seen in Fig. 3. Surprisingly, the below-gap pump excitation of the blend also produces the *same* polaron PA features as those produced with above-gap pump excitation; this confirms that polaron photogeneration is also possible with below-gap pump, in agreement with the transient PM data discussed in Sec. III A above. We emphasize that the mechanism by which the polaron species are photogenerated with below-gap excitation cannot be explained by the known single-step photoinduced charge transfer reaction,<sup>9,10</sup> since singlet excitons that supposedly precede charge dissociation are not photogenerated in the polymer or fullerene domains, as revealed in the picosecond transient PM spectrum (Fig. 2). We invoke that the alternative mechanism of polaron photogeneration with below-gap pump excitation is related with the CTC that is formed at the polymer/fullerene interface.<sup>35</sup>

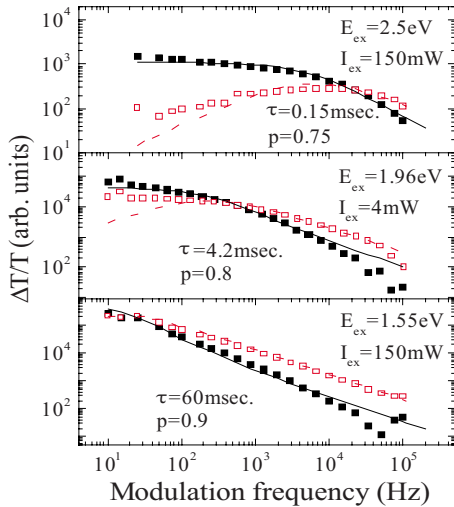


FIG. 4. (Color online) Modulation frequency dependence of the  $P_1$  PA polaron band in RR-P3HT/PCBM blend measured at  $\hbar\omega(\text{probe})=0.4$  eV and  $T=30$  K; both in-phase (full black squares) and quadrature (empty red squares) PA are shown. The lines through the data points are fit using Eq. (1), where the best-fit lifetime,  $\tau$  and dispersive parameter exponent,  $p$  are indicated. The various panels represent different pump excitation  $\hbar\omega$ : top panel is for above-gap excitation pumped at  $\hbar\omega=2.5$  eV; middle panel is for below-gap excitation pump at  $\hbar\omega=1.96$  eV; bottom panel is for below-gap excitation at  $\hbar\omega=1.55$  eV.

To further investigate the process by which polarons are photogenerated with below-gap excitation we studied the polarons recombination dynamics generated with below-gap and above-gap pump excitations. The recombination dynamics was obtained from the modulation-frequency response of the  $P_1$  PA band of the polarons using the bimolecular dispersive recombination model.<sup>51</sup> Figure 4 shows the PA response at temperature  $T=30$  K, and the fit using Eq. (1) from which the lifetime,  $\tau$ , was obtained. We realize that  $\tau$  dramatically increases with below-gap excitation. The increase in  $\tau$  is by about three orders of magnitude, from  $\tau=150$   $\mu\text{s}$  with above-gap pump excitation at  $\hbar\omega=2.5$  eV to  $\tau=60$  ms with below-gap excitation at  $\hbar\omega=1.55$  eV. This shows that below-gap photogenerated polarons *have much slower recombination kinetics*. For the diffusion-limited bimolecular kinetics known to exist in polymers,<sup>52</sup> this indicates either increased localization for the below-gap photogenerated polarons or charge separation into two different phases, namely, the polymer and fullerene domains.

We also used the polaron action spectrum for understanding the below-gap polaron photogeneration process, where we probe the strength of the polaron  $P_1$  band between 0.25–0.4 eV as a function of the excitation  $\hbar\omega$ , normalizing by the impinging excitation photon flux,  $I_L$ . Figure 5(a) shows the polaron action spectra for pristine P3HT and P3HT/PCBM blend. The polaron photogeneration action spectrum of pristine P3HT has a clear onset at the polymer band edge ( $\sim 1.85$  eV); and lacks the below-gap polaron generation component. In contrast, the polaron photogeneration action spectrum in the blend extends to  $\hbar\omega(\text{pump})$  well into the polymer optical gap with an extrapolated onset at  $\hbar\omega \sim 1.2$  eV, i.e., much smaller than the polymer and fullerene

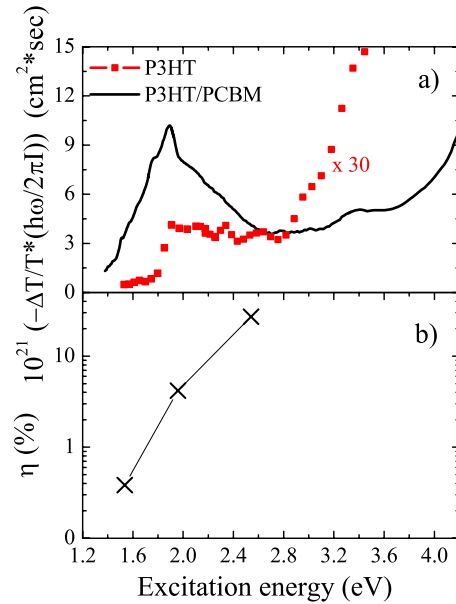


FIG. 5. (Color online) Pump excitation dependence of polarons in RR-P3HT/PCBM blend measured at  $T=30$  K. (a) Polaron band  $P_1$  action spectra for RR-P3HT (squares) and RR-P3HT/PCBM blend (solid line) measured at  $\hbar\omega(\text{probe})$  between 0.25–0.4 eV, normalized to the impinging excitation photon flux. (b) The polaron QE,  $\eta$  for RR-P3HT/PCBM blend obtained from the polaron action spectrum (a) and lifetime (Fig. 4) using Eq. (2), for three different pump excitation  $\hbar\omega$ : namely, 2.5, 1.96, and 1.55 eV.

absorption edges. In addition the polaron action spectrum also shows a prominent peak at  $\sim 1.9$  eV having an apparently smaller polaron generation efficiency for  $\hbar\omega > E_g$  (the polymer optical gap). This is an *illusion*, however, since the polaron lifetime is longer with below-gap excitation. This dramatically influences the polaron action spectrum, since the measurements are done at steady-state conditions, where the polaron density is also influenced by their recombination lifetime. This is verified when we compare the polaron action spectrum to the IPCE spectrum showed in Fig. 6. As we can see there is little collection efficiency for  $\hbar\omega(\text{pump}) < \hbar\omega$

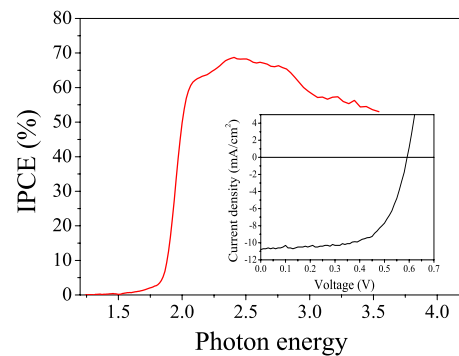


FIG. 6. (Color online) The IPCE spectrum of an OPV device based on the RR-P3HT/PCBM blend. The device  $I$ - $V$  characteristic under solarlike illumination of AM 1.5 is shown in the inset. The estimated device PCE is 4.2% and is in very good agreement with the PCE calculated from the IPCE convoluted with the solar illumination spectrum at AM 1.5.

constituents' gap. This tail, however, may also be influenced by the small thickness ( $\sim 100$  nm) of the active layer in the device.

To correct for this unusual ‘‘lifetime effect’’ in the polaron action spectrum, we calculated the polaron photogeneration quantum efficiency (QE),  $\eta$  using the following relation that is appropriate for an optically thick film:<sup>19,46</sup>

$$-\Delta T/T(\hbar\omega = P_1) = \tau\sigma\eta I_L, \quad (3)$$

where  $\sigma$  is the polaron optical cross section at  $\hbar\omega = P_1$  and  $I_L$  is the normalized excitation intensity. In Eq. (3) we choose  $\sigma = 2 \times 10^{-17}$  cm<sup>2</sup>,<sup>39</sup> and took  $\tau$  from the lifetime measurements described above. The obtained QE of polaron photogeneration using Eq. (3) is shown in Fig. 5(b) for three different pump excitations; the lifetime normalization makes the polaron excitation spectrum to look more similar to the IPCE spectrum (Fig. 6). We see that the apparent peak at 1.9 eV is eliminated now from the steady-state action spectrum. In addition it is also clear that when correcting for the polaron lifetime, then the polaron QE is *lower* for below-gap excitation compared with that for excitation above the gap. This is probably caused by substantial geminate recombination for below-gap excitation.<sup>8</sup> Nevertheless the QE of below-gap-generated polarons is definitely not negligibly small.

The polaron QE value that we obtained here for  $\hbar\omega > E_g$  is somewhat smaller than that extracted from the IPCE (Fig. 6). This may be due to the uncertainty in setting the value of the parameter  $\sigma$  in P3HT [Eq. (3)]. In fact  $\sigma$  depends on the probe  $\hbar\omega$  and follows the  $P_1$  spectrum.  $P_1$ , in turn, peaks at  $\hbar\omega \sim 80$  meV (see Fig. 3), which is outside the experimental probe spectral range (0.25–0.5 eV) that we used here for  $P_1$  in the action spectrum measurement. The calculated  $\eta$  value using Eq. (3) for a higher  $\sigma$  values than for  $\hbar\omega(\text{probe})$  we used here would be significantly higher than the obtained  $\eta$  value in Fig. 5.

### C. Electroabsorption spectroscopy

The mechanism by which below-gap polaron photogeneration occurs without involving exciton formation may be better understood by involving a CTC state at the interface between the polymer and fullerene domains, that lies below the optical gap of the blend material constituents. One viable way to measure such a CTC state is using the EA spectroscopy; since such a state may have a large dipole moment that enhances the EA signal.<sup>27,28</sup> In EA measurements, a change in transmission through the sample due to a modulated applied electric field is obtained. The EA for polymers is measured at  $2f$ , where  $f$  is the field modulation frequency, because of the polymer chain symmetry.<sup>41</sup> We note that the EA spectroscopy has been extensively used in the literature to reveal small optical transitions in polymers that are coupled by a strong dipole transition;<sup>53</sup> and this situation exists in our case since the CTC absorption band may be overwhelmed by the absorption tail in the blend.<sup>13</sup>

The EA spectrum of the pristine RR-P3HT [Fig. 7(a)] is dominated by the strongly coupled exciton transitions  $1B_u$  and  $mA_g$  at 2.0 eV and 2.7 eV, respectively.<sup>39</sup> Whereas the

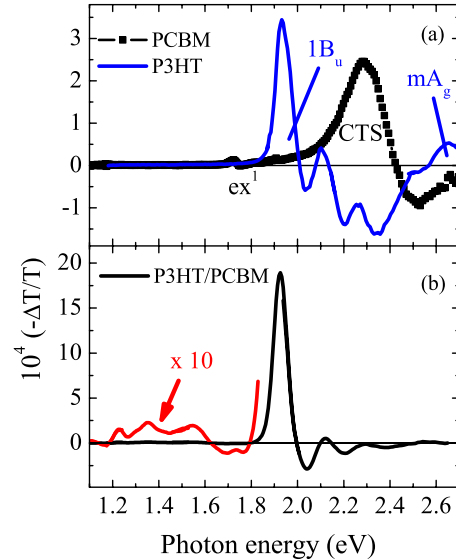


FIG. 7. (Color online) (a) The EA spectra of pristine RR-P3HT (blue line) and PCBM (black squares).  $1B_u$  and  $mA_g$  denote strongly coupled exciton states in the polymer; whereas CTS denotes the charge transfer state in the fullerene. (b) The EA spectrum of RR-P3HT/PCBM blend, where the below-gap spectrum is also shown multiplied by a factor of 10. The CTC in the blend is denoted.

EA spectrum of PCBM reveals the charge transfer state (denoted CTS) transition at 2.4 eV (Ref. 19) in this material. We note that there are no optical EA features below the polymer and fullerene optical gaps for the pristine polymer and fullerene films. In contrast, an EA band with an onset at 1.2 eV is obtained in the blend [Fig. 7(b)]. A broad derivativelike feature can be seen, followed by a broadband that spans  $\hbar\omega(\text{probe})$  range from 1.2 to 1.8 eV with several clear peaks. We assign this new EA feature to the CTC state in the gap and speculate that the various secondary peaks are due to excited states in the CTC manifold. A possible transition from the lowest CTC state to the highest excited state in this manifold, in fact, may explain<sup>28</sup> the transition  $PA'$  that was obtained at  $\sim 0.45$  eV in the picosecond time domain with below-gap pump, discussed above in Sec. III A [see Fig. 2(b)]. We note that although the CTC states are mainly formed at the polymer/fullerene interfaces with relatively small cross section, it is still possible to observe its associated optical transitions using EA spectroscopy due to its strong coupled dipole moment;<sup>28</sup> this can be barely achieved using linear absorption measurements.<sup>13</sup> The EA onset at 1.2 eV, which we interpret here as the onset of the CTC manifold, is the lowest  $\hbar\omega$  obtained for the CTC so far in any blend.<sup>14,24</sup> This may be an important contributing factor for the high PCE of  $\sim 4.2\%$  obtained for the OPV device (Fig. 6) based on the RR-P3HT/PCBM blend.

### IV. SUMMARY

In summary, we investigated the nature of the below-gap CTC states in RR-P3HT/PCBM blend used for photovoltaic applications. The photogeneration of charged polarons using

below-gap pump excitation and their distinguishable different recombination mechanism compared to that of above-gap pump polarons indicate that a charge photogeneration mechanism operates in the blend; this should be seriously considered in analyzing photovoltaic properties of solar-cell devices. The EA spectrum of the blend places the lowest lying CTC state in RR-P3HT/PCBM blend at  $\sim 1.2$  eV, which is much deeper than the CTC state measured thus far in any other polymer/fullerene blends.<sup>13,14</sup> We also measured several excited states in the CTC manifold that may show up in ultrafast PM measurements in the blend.

The primary photoexcitations in the blend with above-gap pump are singlet excitons and polarons in the polymer phase that are generated within our time resolution of 150 fs. The excitons quickly decay within 10 ps, but additional polarons correlated with this decay *are not formed in our time interval*. When exciting the CTC states resonantly using below-gap pump excitation, we obtained excitation species that we interpret as CT excitons. These species decay within 10 ps

into trapped polarons, and this process may explain the steady-state polaron photogeneration with below-gap pump excitation. When comparing the polaron action spectrum with the IPCE spectrum measured on an OPV solar-cell device based on the RR-P3HT/PCBM blend, we conclude that the polarons photogenerated with below-gap pump can contribute to the device photocurrent only when the active layer of the device would be much thicker than the typical 100 nm usually used.

## ACKNOWLEDGMENTS

We thank Darin Laird and Sergey Li from Plextronics for supplying the data for the P3HT/PCBM device and for their generous supply of the RR-P3HT and PCBM constituents. This work was supported in part by the NSF under Grant No. DMR 08-03325 and DOE under Grant No. DE-FG02-04ER46109 at the University of Utah.

\*Present address: Department of Physics, University of California at Berkeley, Berkeley, California 94720.

†Present address: National Renewable Energy Laboratory, Golden, Colorado 80401.

‡Author to whom correspondence should be addressed; val@physics.utah.edu

<sup>1</sup>G. Yu, J. Gao, J. C. Hummelen, F. Wudl, and A. J. Heeger, *Science* **270**, 1789 (1995).

<sup>2</sup>G. Li, V. Shrotriya, J. Huang, Y. Yao, T. Moriarty, K. Emery, and Y. Yang, *Nature Mater.* **4**, 864 (2005).

<sup>3</sup>Y. Kim, S. Cook, S. M. Tuladhar, A. Choulis, J. Nelson, J. R. Durrant, D. D. C. Bradley, M. Gilles, I. McCulloch, C. S. Ha, and M. Ree, *Nature Mater.* **5**, 197 (2006).

<sup>4</sup>J. Peet, J. Y. Kim, N. E. Coates, W. L. Ma, D. Moses, A. J. Heeger, and G. C. Bazan, *Nature Mater.* **6**, 497 (2007).

<sup>5</sup>J. Y. Kim, K. Lee, N. E. Coates, D. Moses, T.-Q. Nguyen, M. Dante, and A. J. Heeger, *Science* **317**, 222 (2007).

<sup>6</sup>S. D. Oosterhout, M. M. Wienk, S. S. van Bavel, R. Thiedmann, L. J. A. Koster, J. Gilot, J. Loos, V. Schmidt, and R. A. J. Janssen, *Nature Mater.* **8**, 818 (2009).

<sup>7</sup>M. A. Green, K. Emery, Y. Hishikawa, and W. Warta, *Prog. Photovoltaics* **17**, 320 (2009).

<sup>8</sup>Y. Liang, Z. Xu, J. Xia, S.-T. Tsai, Y. Wu, G. Li, C. Ray, and L. Yu, *Adv. Mater.* **22**, E135 (2010).

<sup>9</sup>N. S. Sariciftci, L. Smilowitz, A. J. Heeger, and F. Wudl, *Science* **258**, 1474 (1992).

<sup>10</sup>S. Morita, A. A. Zakhidov, and K. Yoshino, *Solid State Commun.* **82**, 249 (1992).

<sup>11</sup>V. I. Arkhipov, P. Heremans, and H. Bässler, *Appl. Phys. Lett.* **82**, 4605 (2003).

<sup>12</sup>A. A. Bakulin, S. G. Elizarov, and A. Khodarev, *Synth. Met.* **147**, 221 (2004).

<sup>13</sup>L. Goris, A. Poruba, L. Hod'áková, M. Vančček, K. Haenen, M. Nesládek, P. Wagner, D. Vanderzande, L. De Schepper, and J. V. Manca, *Appl. Phys. Lett.* **88**, 052113 (2006).

<sup>14</sup>J. J. Benson-Smith, L. Goris, K. Vandewal, K. Haenen, J. V.

Manca, D. Vanderzande, D. D. C. Bradley, and J. Nelson, *Adv. Funct. Mater.* **17**, 451 (2007).

<sup>15</sup>V. V. Bruevich, T. Sh. Makhmutov, S. G. Elizarov, E. M. Nechvolodova, and D. Yu. Paraschuk, *J. Chem. Phys.* **127**, 104905 (2007).

<sup>16</sup>P. Panda, D. Veldman, J. Sweelssen, J. J. A. M. Bastiaansen, B. M. W. Langeveld-Voss, and S. C. J. Meskers, *J. Phys. Chem. B* **111**, 5076 (2007).

<sup>17</sup>W. Osikowicz, M. P. de Jong, and W. R. Salaneck, *Adv. Mater.* **19**, 4213 (2007).

<sup>18</sup>I. W. Hwang, D. Moses, and A. J. Heeger, *J. Phys. Chem. C* **112**, 4350 (2008).

<sup>19</sup>T. Drori, C.-X. Sheng, A. Ndobe, S. Singh, J. Holt, and Z. V. Vardeny, *Phys. Rev. Lett.* **101**, 037401 (2008).

<sup>20</sup>M. Hallermann, S. Haneder, and E. Da Como, *Appl. Phys. Lett.* **93**, 053307 (2008).

<sup>21</sup>P. Parkinson, J. Lloyd-Hughes, M. B. Johnston, and L. M. Herz, *Phys. Rev. B* **78**, 115321 (2008).

<sup>22</sup>A. A. Bakulin, S. A. Zapunidy, M. S. Pshenichnikov, P. H. M. van Loosdrecht, and D. Yu. Paraschuk, *Phys. Chem. Chem. Phys.* **11**, 7324 (2009).

<sup>23</sup>J. Holt, S. Singh, T. Drori, Y. Zhang, and Z. V. Vardeny, *Phys. Rev. B* **79**, 195210 (2009).

<sup>24</sup>M. Hallermann, I. Kriegel, E. Da Como, J. M. Berger, E. von Hauff, and J. Feldmann, *Adv. Funct. Mater.* **19**, 3662 (2009).

<sup>25</sup>J. L. Brédas, D. Beljonne, V. Coropceanu, and J. Cornil, *Chem. Rev.* **104**, 4971 (2004).

<sup>26</sup>Z. D. Wang, S. Mazumdar, and A. Shukla, *Phys. Rev. B* **78**, 235109 (2008).

<sup>27</sup>H. Alves, A. S. Molinari, H. X. Xie, and A. F. Morpurgo, *Nature Mater.* **7**, 574 (2008).

<sup>28</sup>K. Aryanpour, D. Psiachos, and S. Mazumdar, *Phys. Rev. B* **81**, 085407 (2010).

<sup>29</sup>D. Veldman, S. C. J. Meskers, and R. A. J. Janssen, *Adv. Funct. Mater.* **19**, 1939 (2009).

<sup>30</sup>C. J. Brabec, N. S. Sariciftci, and J. C. Hummelen, *Adv. Funct.*



- Mater.* **11**, 15 (2001).
- <sup>31</sup>W. L. Ma, C. Y. Yang, X. Gong, K. H. Lee, and A. J. Heeger, *Adv. Funct. Mater.* **15**, 1617 (2005).
- <sup>32</sup>A. J. Moulé and K. Meerholz, *Adv. Mater.* **20**, 240 (2008).
- <sup>33</sup>Y. Gao and J. K. Grey, *J. Am. Chem. Soc.* **131**, 9654 (2009).
- <sup>34</sup>P. E. Shaw, A. Ruseckas, and I. D. W. Samuel, *Adv. Mater.* **20**, 3516 (2008).
- <sup>35</sup>R. Mondal, S. Ko, J. E. Norton, N. Miyaki, H. A. Becerril, E. Verploegen, M. F. Toney, J.-L. Brédas, M. D. McGehee, and Z. Bao, *J. Mater. Chem.* **19**, 7195 (2009).
- <sup>36</sup>R. A. Marsh, J. M. Hodgkiss, S. Albert-Seifried, and R. H. Friend, *Nano Lett.* **10**, 923 (2010).
- <sup>37</sup>C.-X. Sheng, M. Tong, S. Singh, and Z. V. Vardeny, *Phys. Rev. B* **75**, 085206 (2007).
- <sup>38</sup>T. Drori, E. Gershman, C.-X. Sheng, Y. Eichen, Z. V. Vardeny, and E. Ehrenfreund, *Phys. Rev. B* **76**, 033203 (2007).
- <sup>39</sup>R. Österbacka, C. P. An, X. M. Jiang, and Z. V. Vardeny, *Science* **287**, 839 (2000).
- <sup>40</sup>O. Epshtein, G. Nakhmanovich, Y. Eichen, and E. Ehrenfreund, *Phys. Rev. B* **63**, 125206 (2001).
- <sup>41</sup>M. Liess, S. Jeglinski, Z. V. Vardeny, M. Ozaki, K. Yoshino, Y. Ding, and T. Barton, *Phys. Rev. B* **56**, 15712 (1997).
- <sup>42</sup>S. V. Frolov, Z. Bao, M. Wohlgenannt, and Z. V. Vardeny, *Phys. Rev. B* **65**, 205209 (2002).
- <sup>43</sup>O. J. Korovyanko, R. Österbacka, X. M. Jiang, Z. V. Vardeny, and R. A. J. Janssen, *Phys. Rev. B* **64**, 235122 (2001).
- <sup>44</sup>It may be due to photoexcitations related to excimers, K. Aryanpour, C.-X. Sheng, D. Psiachos, E. Olejnik, B. Pandit, S. Mazumdar, and Z. V. Vardeny (unpublished).
- <sup>45</sup>H. Sirringhaus, P. J. Brown, R. H. Friend, M. M. Nielsen, K. Bechgaard, B. M. W. Langeveld-Voss, A. J. H. Spiering, R. A. Janssen, E. W. Meijer, P. Herwig, and D. M. de Leeuw, *Nature (London)* **401**, 685 (1999).
- <sup>46</sup>T. Drori, Ph.D. thesis, University of Utah, 2008.
- <sup>47</sup>M. G. Harrison, K. E. Ziemelis, R. H. Friend, P. L. Burn, and A. B. Holmes, *Synth. Met.* **55**, 218 (1993).
- <sup>48</sup>Y.-S. Huang, S. Westenhoff, I. Avilov, P. Sreearunothai, J. M. Hodgkiss, C. Deleener, R. H. Friend, and D. Beljonne, *Nature Mater.* **7**, 483 (2008).
- <sup>49</sup>S. Westenhoff, I. A. Howard, J. M. Hodgkiss, K. R. Kirov, H. A. Bronstein, C. K. Williams, N. C. Greenham, and R. H. Friend, *J. Am. Chem. Soc.* **130**, 13653 (2008).
- <sup>50</sup>R. Österbacka, X. M. Jiang, C. P. An, B. Horovitz, and Z. V. Vardeny, *Phys. Rev. Lett.* **88**, 226401 (2002).
- <sup>51</sup>O. Epshtein, Y. Eichen, E. Ehrenfreund, M. Wohlgenannt, and Z. V. Vardeny, *Phys. Rev. Lett.* **90**, 046804 (2003).
- <sup>52</sup>L. J. A. Koster, V. D. Mihailetschi, and P. W. M. Blom, *Appl. Phys. Lett.* **88**, 052104 (2006).
- <sup>53</sup>L. Sebastian and G. Weiser, *Phys. Rev. Lett.* **46**, 1156 (1981).